

DESIGN AND TEST OF SUPPLEMENTAL FEEDING PUSHER DEVICE FOR CATTLE STABLE

牛场补饲推料装置设计与试验

Yumeng XIAO¹), Taowei JIAO¹), Wenjie ZHAO¹), Hengxu ZHU¹), Hongming ZHANG²), Pengpeng SUN²), Wei LI^{*1})

¹) Northwest A&F University, College of Mechanical and Electronic Engineering/ China;

²) Northwest A&F University, College of Information Engineering/China

Tel: +86-139-0925-8177; E-mail: liweizibo@nwsuaf.edu.cn

DOI: <https://doi.org/10.35633/inmateh-73-22>

Keywords: livestock machinery; design; beef cattle; assisted feeding; auger; push feeder

ABSTRACT

This paper proposed a supplemental feeding pusher based on beef cattle's auxiliary feeding needs to solve the traditional feeding mode of manual work, labor intensity, and inconsistent manual work standards. Firstly, the conveyed feed particles movement process was established as a motion model and the basis of the design parameters of the screw conveyor was explained. ANSYS static analysis module was used to ensure that the structural parameters of the discharging device were reasonable, ANSYS vibration modal analysis module was used to verify the frame strength and stability. According to the theoretical design of the trial prototype, the control system with STM32F103RE microcontroller as the core was carried out. Finally, the orthogonal test was conducted with the screw shaft speed, sweeping roller brush height, and traveling speed as test factors; different parameters were set to verify the effect of supplemental feeding and pushing, and parameter optimization of the test results was carried out using Design-Expert software. The optional combination of working parameters was determined to be the feeding screw shaft speed 188 r/min, the sweeping roller brush speed 160 r/min, and the work speed 0.26 m/s. The test demonstrated that the residual feed width was 0.73 m, and the transverse coefficient of variation was 14.9%, which could satisfy the needs of auxiliary feeding for beef cattle. This study reduced feed waste and met the cattle feeding needs to the greatest extent, and it could provide a reference for auxiliary feeding machinery.

摘要

为解决传统饲喂方式以人工作业为主、劳动强度大、作业标准不统一且效率低的问题，本文基于肉牛辅助饲喂需求设计了一种的补饲推料机。首先，对输送的饲料颗粒运动过程建立运动模型并说明螺旋输送装置设计参数依据，利用 ANSYS 静力学分析模块确保下料装置结构参数合理，并利用 ANSYS 振动模态分析模块验证机架强度和稳定性；根据理论设计试制样机，对以 STM32F103RE 单片机为核心的补料清扫控制系统进行了设计。最后，以螺旋轴转速、清扫滚刷高度、行驶速度为试验因素进行正交试验，设置不同参数验证补饲推料效果，使用 Design-Expert 软件对试验结果进行参数优化，结果表明，当送料螺旋轴转速为 188 r/min，清扫滚刷转速为 160 r/min，行进速度为 0.26 m/s 时，余料幅宽为 0.73 m，横向变异系数为 14.9%，能够满足肉牛辅助饲喂的需求该研究减少了饲料的堆积浪费，最大程度上满足动物的采食需求，可为辅助饲喂机械的设计优化提供参考。

INTRODUCTION

With the development of science and technology empowering the beef cattle breeding industry, feeding methods are constantly changing from traditional feeding methods to TMR methods at this stage (Zhong et al., 2020), but most beef cattle farms currently have a low degree of automation (Bae et al., 2023). During the feeding process of beef cattle, it often happens that straw and other remaining roughage accumulated in the trough or the grass is arched away from the feeding area due to the preference for concentrate feed (Greter et al., 2015), resulting in a decline in cattle intake and feed waste (Da Borso et al., 2017).

The traditional solution is to sweep scattered feed manually or drive the feed truck to push the remnant feed, which is inefficient, and the operation effect cannot be effectively guaranteed. If scattered feed is not pushed back promptly, it may lead to a buildup of fermentation, affecting the stable environment and cattle health (Nabokov et al., 2020; Liu et al., 2016). Cattle's feeding and living environment directly affect their growth conditions (Tangorra and Calcante, 2018; Moya et al., 2011). In the long run, it not only causes the waste of feed but also affects the cattle quality (Cummins et al., 2009) and reduces the economic value (Álvarez-Rodríguez et al., 2020), so the research on assisted feeding robots has been generated (Pavkin et al., 2023).

Auxiliary feeding equipment like supplemental feeding equipment and pushing machinery is an essential part of intelligent farming (Alameer *et al.*, 2020; Pavkin *et al.*, 2021), which can improve the efficiency of feed utilization as well as the eating quality of beef cattle (Mosquera *et al.*, 2021; Bisaglia, 2012). Many researchers have recently focused on automated feeding robots (Bisaglia, 2023; Yang *et al.*, 2022). Uzedhe *et al.* presented an on-farm automated feeding robotic system that consisted of automatic navigation, which could provide 26.6 kg of feed automatically at 1.233 km/h, but it was incapable of tipping and pushing loose material and was not suitable for automatic feeding of beef cattle (Uzedhe *et al.*, 2023). The cow intelligent pushing robot developed by Zhang *et al.* used a straight-faced pushing plate to push the material and acquired images through a webcam; however, the recognition rate of this method for the QR code was easily affected by environmental factors (Zhang *et al.*, 2023). Chen *et al.* used the 9ITL-650 feeding robot as a platform and constructed an ultra-wideband autonomous navigation system, but the device had a single function, and it could not satisfy the replenishment feeding as well as sweeping and other operations (Chen *et al.*, 2024). Bakirov *et al.* developed a robotic control system for cattle shed feeding and carried out an operational procedure that allowed for automated feeding of typical cattle yards. However, it lacked pushing and sweeping functions to meet complete automation requirements (Bakirov *et al.*, 2020).

In summary, due to the problem of frequent replenishment and pushing of materials in beef cattle farms, there is a lack of an integrated cattle farm auxiliary feeding machine that can simultaneously realize automatic replenishment, moving materials, and cleaning. Considering the problems of existing feeding machinery, a structure and working method of a supplemental feeding pusher are proposed. Automatically achieving timely replenishment, pushing, and cleaning can solve the problem of low grass utilization as it is removed from the feeding area by the cattle.

MATERIALS AND METHODS

Machine structure and working principle

Structure of supplemental feeding pusher

The supplemental feeding pusher consists of the traveling chassis, discharging device, sweeping device, power supply, navigation module and central control module. As shown in Fig. 1, the device can push back the feed along the feed routing trajectory to facilitate beef cattle feeding. At the same time, it carries a silo that can add following the remaining feed in the process of the feeding of the beef cattle. For the operating environment of beef farms, the traveling chassis is steered by the front axle and driven by the rear axle, and the system adopts the UWB (ultra-wide band) positioning mode and integrates the IMU (micro-inertial measurement unit) data information for navigation. Considering loose-feeding as the mainstream of livestock breeding, the application scenario of the designed supplemental feeding pusher is loose-feeding mode, with an open range of cattle activities and fixed feeding points.

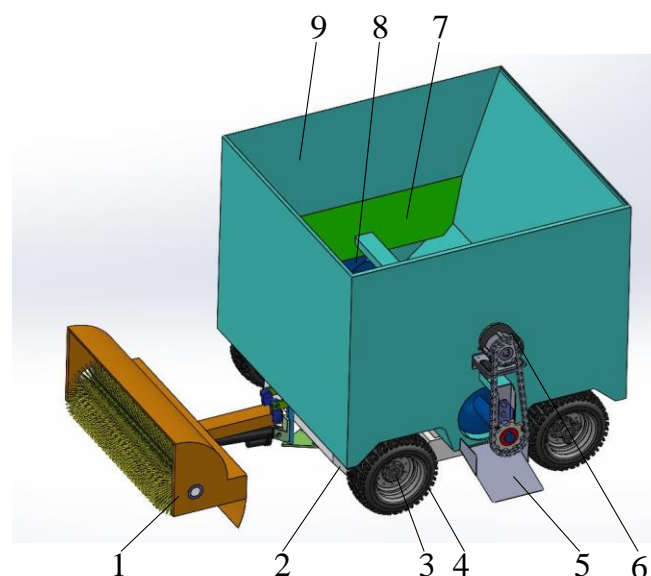


Fig. 1 - Structure of the supplemental feed pusher

1. Cleaning device; 2. Frame; 3. Wheel encoder; 4. Rolling wheel; 5. Feeding plate;
6. Motor; 7. Leak-proof baffle; 8. Feeding screw; 9. Silo

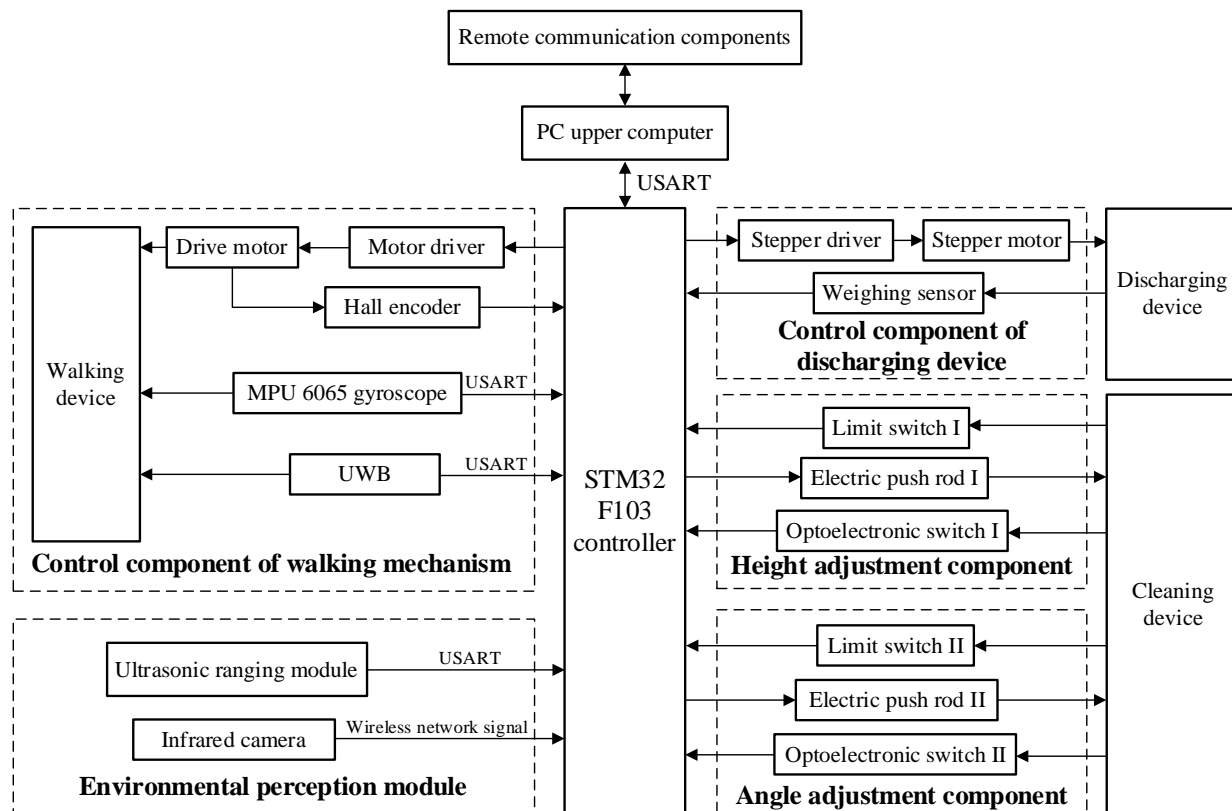


Fig. 2 - Overall control system diagram for the supplemental feeding pusher

The microcontroller integrates microprocessor, memory and other parts to form a miniature computing system, with reliability and fast operation advantages. Given the beef cattle feeding requirements, the composition of the hardware part of the supplemental feeding pusher control system is determined. The STM32F103 microcontroller is the total controller of the whole system, which is connected to the ultrasonic range sensor, load cell and other modules. The overall control system diagram for the supplemental feeding pusher is shown in Fig. 2.

Working principle and technical parameters

According to the requirements of the beef cattle breeding feeding link, firstly, the TMR (total mixed ration) spreading wagon completes the feed sprinkling in the stable. After 1.5 h of centralized feeding by the spreading wagon, the supplemental feeding pusher carries out the pushing and supplemental feeding operation. The working method of the designed supplemental feeding pusher system is as follows: after turning on the power supply unit, it makes a fixed stop at the starting point A position, and then through the system distance measuring sensor, the distance to the cattle neck yoke railings is measured.

After entering the area to be operated, stop at the starting point A position, measure the distance to the border cattle neck yoke fence through the system distance measuring sensor, adjust the distance between the left and right of the AB section, and get ready to enter the working state. After entering the feeding area through the B point, monitor the distance to the border cattle neck yoke fence in real time in the process of the straight operation of the BC section, and control the distance from the border to a certain extent.

During the operation of the feeding area, set up a suitable working mode in advance, and the supplementary feeding pusher will carry out the supplementary feeding and cleaning operation; after completing the operation of one side of the feeding area, it will drive to the cattle house D. After finishing the work in the feeding area on one side, it will drive to the D section of the stable, turn at the DE section at the end of the stable, and complete the pushing and feeding operation on the other side. The main technical parameters of the supplemental feed pusher are shown in Table 1.

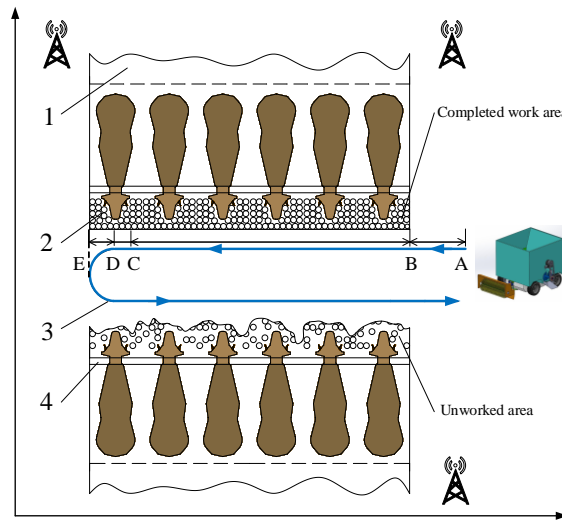


Fig. 3 - Schematic diagram of the operation of the supplemental feeding pusher
 1. Beef cattle activity area; 2. Feeding area; 3. Operating track; 4. Neck yoke

Table 1

Main technical indexes of feeding pusher	
Parameters	Values
Overall dimensions (lengthx widthx height) /mmx mmx mm	1350×1200×1450
Quantity of material in storage /m ³	3.2
Silo Flow Pattern	Integral flow
Operating speed /(m/s)	≤0.4
Weight /kg	165

Design and analysis of supplemental feeding pusher components

Design and simulation verification of discharging device

In order to realize the supplemental forage function of the supplemental feed pusher, it is required that the feed stored in the silo can be uniformly and steadily fed to the feeding area. The feeding device mainly consists of a silo, conveying screw, anti-leakage baffle, motor, weighing device and other parts, as shown in Figure 4. The screw conveyor has the advantages of simple structure and reliable work, and it is easy to control frequency in the actual production. By selecting different motor speeds, it is easier to control the amount of feed accurately. To avoid the problem of "hygroscopic agglomeration" caused by the accumulation of feed in the silo for too long a period, a side length of 1200 mm square funnel-type silo is used. When working, the motor drive conveyor screw rotates through the chain, through the guide plate to avoid uneven feeding and clogging phenomenon, and then fall into the conveyor screw blade. The feed plate has a tilt angle to ensure that the feed is thrown to the scope of the feeding area. When discharging is stopped, the motor stops, and the remaining forage in the silo can be a leakage barrier to block to avoid wastage.

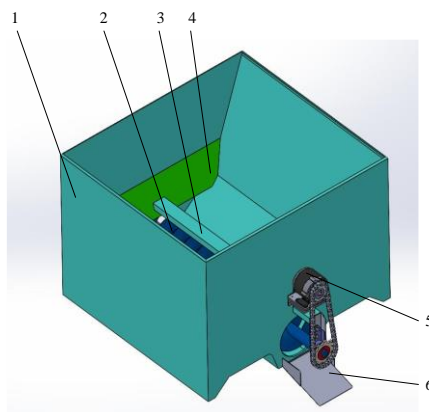


Fig. 4 - Structure of the discharging device

1. Bin; 2. Feeding screw; 3. Guide plate; 4. Leak-proof baffle; 5. Motor; 6. Feeding plate

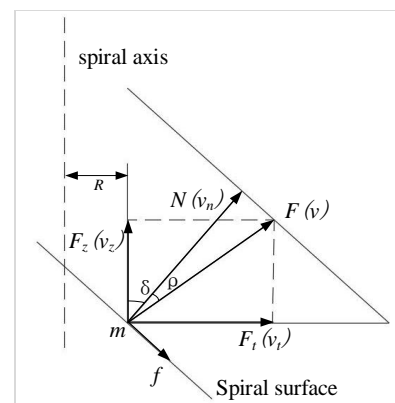


Fig. 5 - Mechanical and kinematic decomposition of the conveying medium

Theoretical analysis of the process of material transfer in the discharging device is made, and the following assumptions are put forward: it is assumed that the material filling coefficient in the spiral discharging device was the same, without considering the compression of the material in the spiral. Take the material at the distance R from the axis as the object of study, and the force and motion decomposition of the mass point m is shown in Figure 5. It can be seen that v_n is the velocity of the point m along the direction normal to the helical surface, and due to the existence of friction between the material and the helical blades, v is the actual speed of the point m . The helical lift angle of the feeding screw is expressed according to the equation (1).

$$\tan\delta = \frac{S}{\pi D_m} \quad (1)$$

where:

δ is the helical lift angle at which the mass point m is located at that position, [°];

D_m is the diameter at which the mass point m is located at that position, [m];

S is the pitch of the spiral, [m].

In the force decomposition of Fig. 5, the axial force and circumferential force are expressed according to equation (2):

$$\begin{cases} F_t = F \sin(\rho + \delta) \\ F_z = F \cos(\rho + \delta) \end{cases} \quad (2)$$

where:

F is the combined force exerted on the mass m , [N];

F_z is the axial component forces exerted on the mass, [N];

F_t are the circumferential component forces exerted on the mass, [N];

δ is the helical lift angle at which the mass point m is located at that position, [°];

ρ is the equivalent friction angle, approximating the v and v_n deviation amount, [°].

From equations (1) and (2), it can be seen that with the increase of δ , F_z decreases while F_t increases, and the main movement of the conveyed material gradually becomes rotary around the axis. According to the structure of the screw conveying device and the relevant parameters, take out the diameter of the mouth of the material is 275 mm, the diameter of the helical blade is 200 mm, and S is 135 mm.

The simplified 3D model was imported into ANSYS to verify the stability of the discharging device. The simplified 3D model was imported into ANSYS to analyze the force situation and simulate the deformation and stress situation of the feeding screw. The analysis results are shown in Fig. 6.

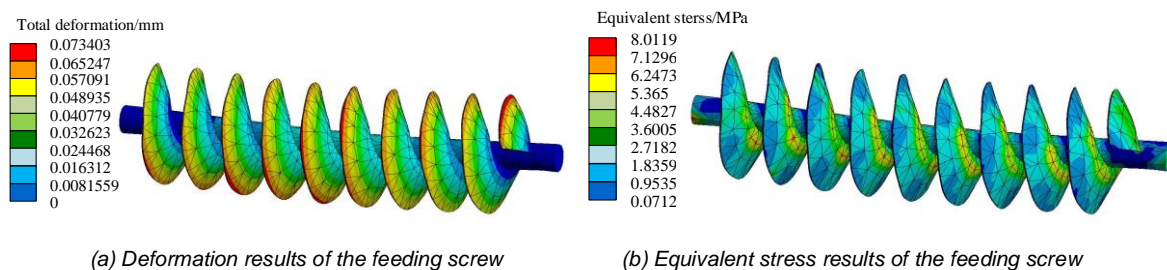


Fig. 6 - Analysis results of the feeding screw

According to the results in Fig. 6(a), the screw was deformed under the action of self-weight, torsional moment and material transfer. The main deformation area was the spiral blade and intermediate shaft position. The maximum deformation is 0.073403 mm, which occurred at the maximum radius of the spiral blade at both ends. The deformation of the edge of the spiral blade was more significant than that at the root position. In Fig. 6(b), the stress of the feeding screw was concentrated in the contact position of the screw blade and the screw shaft. The stress was gradually dispersed and reduced with the increase of the screw radius, and the maximum stress was far less than the yield strength of Q235 235MPa. After analyzing and verifying, the discharging device structure can meet the strength requirements.

Structural design of the cleaning device

The cleaning device can quickly complete the directional sweeping operation of scattered feed, mainly including sweeping brush, brush groove, roller motor and electric actuator. The structure is shown in Fig. 7.

Brush strips are arranged on the periphery of the motor, and the feed left from the gap between the brush clusters in the front row can be cleaned by the brush clusters in the back row, which can prevent the incomplete cleaning phenomenon. In addition, the cleaning brush tufts are installed in the brush groove so they can be replaced after long-term use, reducing maintenance costs. This structural form can realize the collection and discharge of materials and complete both circumferential tangential sweeping and axial pushing during operation.

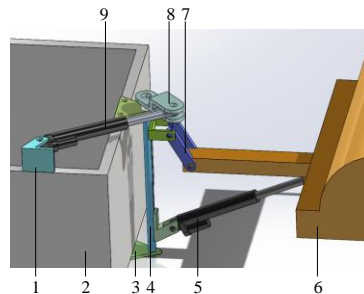


Fig. 7 - Sketch of the structure of the cleaning device

1. Mounting bracket; 2. Frame; 3. Fixed plate; 4. Centre shaft; 5. Electric actuator 1; 6. Brush roller; 7. Connecting plate; 8. Rotating bracket; 9. Electric actuator 2

To improve the feed pushing rate, the height position and working angle of the sweeping device can be controlled by the electric actuator 1 and the electric actuator 2 to complete the sweeping operation of the feed in different directions so that the lower edge of the sweeping brush is in close contact with the ground. When the cleaning device is not working, the vertical direction is raised by 0~70 mm, the lower edges of the cleaning brush and dust cover are not in contact with the ground, and the cleaning device is restored to the initial position.

Vehicle structure design and simulation verification

The frame is integral to the connection between the various working parts. During operation, it is subjected to dynamic loads and vibration from other working parts. When the frequency of the external vibration source and the inherent frequency of the frame are close to, or even coincide with, it is easy to produce damage to the parts. Therefore, modal analysis is used to determine the vibration characteristics of the frame to avoid resonance phenomena and to ensure the reliability of the feeding pusher.

The vibration differential equation of the system during the working process of the supplemental feeding and pushing device, with no external changing load on the frame and ignoring the damping effect, is shown in equation (3):

$$[M]\{x''\} + [K]\{x\} = \{0\} \tag{3}$$

where: $[M]$ is the mass matrix of the frame;

$[K]$ is the stiffness matrix of the frame;

$\{x''\}$ is the acceleration vector matrix;

$\{x\}$ is the displacement vector matrix;

The modal analysis of the frame was carried out using ANSYS Workbench. Generally, the low-order vibration mode plays a relatively important role in the working device, so the transverse axis of the first six orders of the mode of the intrinsic frequency and vibration mode were considered. The modal analysis result is shown in Table 2, and the modal vibration pattern is shown in Figure 8.

Table 2

Rack modal analysis results			
Modal order	Intrinsic frequency (Hz)	Relative deformation peak(mm)	Description of the vibration pattern
1	15.398	2.288	Bend around the X axis
2	31.215	3.082	Bend around the Z axis
3	37.198	3.196	Bend around the Z axis
4	53.055	2.865	Bend around the Y axis
5	60.657	3.182	Bend around the X axis
6	66.606	3.425	Bend around the Y axis

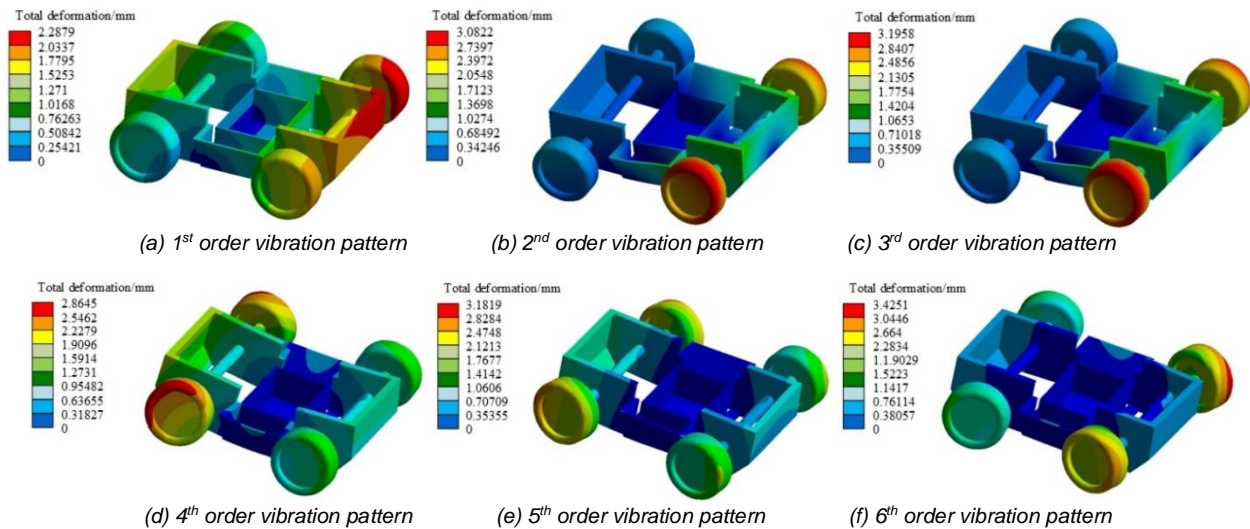


Fig. 8 - The first six orders of the modal vibration pattern of the frame

As seen from Fig. 8, the areas where larger amplitude and deformation occurred were the front and rear ends of the frame, and the deformation inside the frame was minor. The frame carried the weight of the discharging device, and it was affected by the vibration of the discharging device and the sweeping device when they were working, which concentrated the force and vibration in the position of the two ends of the rack, resulting in poor stability. The maximum speed of the drum motor was 5.67 r/s, and the vibration frequency generated by the external stimulation was less than the minimum frame inherent frequency, so the frame would not resonate with other parts during the working process. The structural design is reasonable and meets the stability requirements.

RESULTS

Feeding pusher performance experiment

Experimental conditions

The selected test site was in Yangling District, Shaanxi Province (34°28'N, 108°07'E). The test instruments and materials included a 48 V battery, I/O module terminals, Mini3sPlus UWB module, MPU9250 gyroscope, E3F-DS304C photoelectric switch, HC-SR04 ultrasonic sensor, E6B2-CWZ6 encoder, tape measure, and vernier caliper.

Discharge test

Orthogonal experimental design

According to the theoretical analysis of each working part in the previous period, it was determined that the main factors affecting the working effect of the supplemental feeding pusher were the screw shaft rotation speed, the roller brush rotation speed and the traveling speed as the test factors. Ten 5 m×3 m measurement areas were taken in the test stable. The distance of scattered feed from the cattle neck yoke in each region was measured before the test as the initial offset μ_0 . The residual feed width and uniformity were taken as the test indexes, in which the residual feed width could be measured directly, and the transverse coefficient of variation illustrated the uniformity, and the calculation is shown in equation (4).

$$\begin{cases} CV = \frac{\sigma}{\mu} \\ \sigma = \sqrt{\frac{1}{n-1} \sum_{i=1}^n (\mu_i - \mu_0)^2} \end{cases} \quad (4)$$

where:

- CV is the transverse coefficient of variation, [%];
- σ is the standard deviation;
- n is the number of sampling areas;
- μ_i is the average distance of the residual feed in the i sampling area after the operation, [m];
- μ is the average of μ_i , [m].

Experimental program and results

In order to avoid material accumulation on the inner wall of the silo, the proposed screw shaft speed range was 150 r/min~220 r/min; with reference to the working parameters of similar machinery, the preliminary selection of the sweeping roller brush speed range was 120 ~200 r/min; the proposed range of traveling speeds of the supplemental feeding pusher was 0.1~0.4 m/s. The orthogonal test was used to study the influence of each factor on the machine, and the code levels of factors are shown in Table 3.

Table 3

Test Code and levels of factors			
Code	Test factors		
	Feeding screw shaft speed, x_1 / (r/min)	Sweeping roller brush speed, x_2 / (r/min)	Traveling speed, x_3 / (m/s)
+1.682	220	200	0.4
+1	205.8	183.8	0.34
0	185	160	0.25
-1	164.2	136.2	0.16
-1.682	150	120	0.1

The test was conducted according to the test factors in Table 3, the test and measurement process shown in Fig. 9, and the test results in Table 4.



Fig. 9 - Supplemental feeding pusher discharging test

(a) Test Scene

(b) Measurement process

Table 4

Experimental results					
No	Test factors			Y (m)	CV (%)
	x_1 (r/min)	x_2 (r/min)	x_3 (m/s)		
1	164.2	136.2	0.16	1.08	19.2
2	205.8	136.2	0.16	0.87	17.6
3	164.2	183.8	0.16	1.12	16.2
4	205.8	183.8	0.16	0.95	15.8
5	164.2	136.2	0.34	0.96	17.5
6	205.8	136.2	0.34	0.98	15.9
7	164.2	183.8	0.34	1.02	15.3
8	205.8	183.8	0.34	1.08	14.7
9	150	160	0.25	1.05	17.0
10	220	160	0.25	1.07	14.1
11	185	120	0.25	0.80	19.1
12	185	200	0.25	0.91	14.0
13	185	160	0.1	1.04	18.6
14	185	160	0.4	0.90	14.9
15	185	160	0.25	0.62	14.5
16	185	160	0.25	0.73	13.7
17	185	160	0.25	0.66	14.9
18	185	160	0.25	0.71	13.8
19	185	160	0.25	0.79	15.1
20	185	160	0.25	0.87	15.0
21	185	160	0.25	0.76	14.5
22	185	160	0.25	0.89	15.2
23	185	160	0.25	0.71	14.8

Analysis of test results

Multiple regression was fitted to the results using Design-Expert 13.0 software to obtain the regression equations for the residual material distance from the neck yoke width Y and the transverse coefficient of variation CV , respectively. It could test the effect of each test factor on the significance of the model.

(1) Residual feed width from the cattle yoke Y

According to the results of the ANOVA, the model $F=7.37$ indicated that the model was significant. For the grading accuracy of the test indicators, the order of influence of the test factors and the interactions between the factors was $x_1^2, x_3^2, x_2^2, x_1x_3, x_2, x_1, x_3, x_1x_2, x_2x_3$, where x_1^2, x_3^2 had a highly significant influence; x_2^2 had a significant influence; x_1x_3 had a slightly significant; $x_2, x_1, x_3, x_1x_2, x_2x_3$ had no significant impact.

The non-significant factors were removed and re-analyzed by ANOVA to obtain the regression equation of each experimental factor on the residual feed distance from the neck yoke width Y according to equation (5) and the results are presented in table 5:

$$Y = 0.7482 + 0.0575x_1x_3 + 0.1168x_1^2 + 0.0443x_2^2 + 0.0850x_3^2 \tag{5}$$

Table 5

Results of ANOVA for residual feed distance from cattle neck yoke width					
Source	Sum of squares	Degree of freedom	Mean square	F	P
Modal	0.4107	9	0.0456	7.37	0.0008***
x_1	0.0052	1	0.0052	0.8392	0.3763
x_2	0.0158	1	0.0158	2.56	0.1338
x_3	0.0034	1	0.0034	0.5491	0.4719
x_1x_2	0.0008	1	0.0008	0.1292	0.7250
x_1x_3	0.0265	1	0.0265	4.27	0.0592*
x_2x_3	0.0002	1	0.0002	0.0323	0.8601
x_1^2	0.2168	1	0.2168	35.23	< 0.0001***
x_2^2	0.0321	1	0.0321	5.05	0.0427**
x_3^2	0.1148	1	0.1148	18.55	0.0009***
Residual	0.0805	13	0.0062		
Lack of fit	0.0162	5	0.0032	0.4029	0.8342
Error	0.0643	8	0.0080		
Total	0.4912	22			

Note: *** denotes highly significant, ** denotes significant, * denotes slightly significant, same as Table 6

(2) Transverse coefficient of variation

According to the ANOVA results, the model $F=19.59$ indicated that the model was significant. For the transverse coefficient variation, the order of magnitude of the effects of the test factors and the interactions between the factors on it were $x_1, x_3, x_3^2, x_2^2, x_2, x_1^2, x_1x_2, x_2x_3, x_1x_3$, where $x_1, x_2, x_3, x_2^2, x_3^2$ had a highly significant influence; x_1x_2, x_1x_3, x_2x_3 had no significant influence. The non-significant factors were removed and re-analyzed by ANOVA to obtain the regression equation of each experimental factor on the transverse coefficient variation according to equation (6) and the results are presented in table 6:

$$CV = 14.61 - 0.6647x_1 - 1.23x_2 - 0.8510x_3 + 0.3610x_1^2 + 0.7146x_2^2 + 0.7853x_3^2 \tag{6}$$

Table 6

Results of ANOVA for transverse coefficient variation					
Source	Sum of squares	Degree of freedom	Mean square	F	P
Modal	170.84/168.38	9	6.35	19.59	< 0.0001***/< 0.0001***
x_1	57.13	1	6.03	18.62	0.0008***
x_2	6.03	1	20.61	63.62	< 0.0001***
x_3	9.89	1	9.89	30.53	< 0.0001***
x_1x_2	0.6050	1	0.6050	1.87	0.1949

Source	Sum of squares	Degree of freedom	Mean square	F	P
X_1X_3	0.0050	1	0.0050	0.0154	0.9030
X_2X_3	0.2450	1	0.2450	0.7562	0.4003
X_1^2	2.07	1	2.07	6.39	0.0252**
X_2^2	8.11	1	8.11	25.04	0.0002***
X_3^2	9.80	1	9.80	30.24	0.0001***
Residual	1.84	5	1.24		
Lack of fit	2.37	8	0.2961	1.24	0.3722
Error	4.21	13	0.3240		
Total	61.35	22			

Response surface analysis

The experimental results were analyzed by Design-Expert 13.0 software to derive the response surfaces of the significant interactions of feeding screw shaft speed x_1 , sweeping roller brush speed x_2 and travel speed x_3 on the residual feed width Y and transverse coefficient of variation CV as shown in Figure 10.

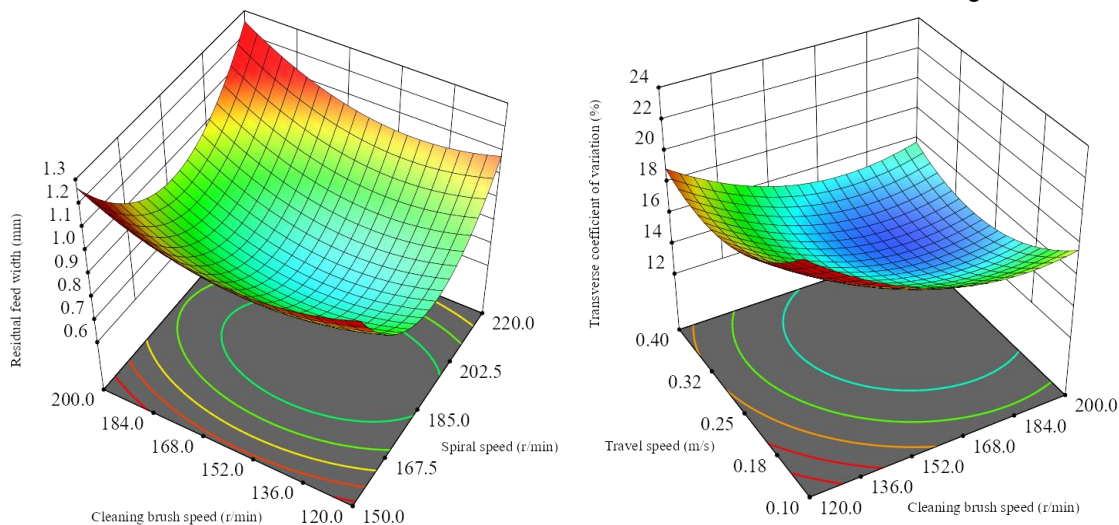


Fig. 10 - Response surface for the interaction between residual feed width and transverse coefficient of variation
(a) $x_3=0.4$ m/s (b) $x_1=185$ r/min

When the traveling speed = 0.4 m/s, the response surface of the interaction between the screw shaft rotation speed and the sweeping brush rotation speed is shown in Fig. 10(a). When the sweeping brush rotation speed was certain, the residual material width showed a decreasing and increasing trend with the increase of the screw shaft rotation speed. The screw rotation speed of the feeding screw influenced the discharged amount and the movement of the material when it was thrown out. The horizontal initial velocity of feed particles was easy to pile up in the non-feeding zone when the screw shaft rotation speed was too low, but when the rotational speed was too high, the discharged amount increased, so the preferred rotational speed of the screw shaft was in the range of 185.0-202.5 r/min. When the rotational speed of the screw shaft was certain, the residual material width showed a decreasing and then increasing tendency with the increasing rotational speed of the sweeping brush. The preferred rotational speed range of the sweeping brush was in the range of 136.0-168.0 r/min.

When the rotational speed of the spiral axis = 185 r/min, the response surface of the interaction between the sweeping brush speed and traveling speed is shown in Fig. 10(b). When the traveling speed was certain, the CV showed a decreasing trend as the speed of the sweeping brush increased and was gradually flattened out because the sweeping brush affected the total amount of pushed feed per unit of time, increasing the efficiency of sweeping. But when the sweeping brush speed exceeded a specific range, the vibration of the whole machine caused by the sweeping device increased, so the optimal range of the sweeping brush speed was 152.0~184.0 r/min; when the speed of the sweeping brush was certain, the CV showed a decreasing and then increasing trend with the increase of the traveling speed, and the better traveling speed was 0.25~0.32 m/s.

Parameter optimization

To obtain the best operational performance parameters of the supplemental feed pusher, the regression model was optimized based on the obtained test results and regression equations with the constraints.

The system of objective and constraint equations is shown in equation (7):

$$\begin{cases} \min Y(x_1, x_2, x_3) \\ \min CV(x_1, x_2, x_3) \\ 150r/min \leq x_1 \leq 220r/min \\ 120r/min \leq x_2 \leq 200r/min \\ 0.1m/s \leq x_3 \leq 0.4m/s \end{cases} \quad (7)$$

The optimal solution was 187.6 r/min for the feeding screw shaft, 160.8 r/min for the sweeping roller brush, and 0.26 m/s for the traveling speed. The residual feed from the cattle neck yoke after the operation of the supplemental feeding push device was 0.71 m in width, with a transverse coefficient of variation of 14.3%.

Experimental validation

Considering the optimized working parameters and operational feasibility, the feeding screw shaft speed was set at 188 r/min, the sweeping roller brush speed at 160 r/min, and the travel speed at 0.26 m/s for the test. The other test conditions were the same as above, and the test results are shown in Table 7.

Table 7

Effectiveness of feeding pusher operation at optimum parameters					
No.	Test factors			Y (m)	CV (%)
	x_1 (r/min)	x_2 (r/min)	x_3 (m/s)		
1	188	160	0.26	0.70	15.9
2	188	160	0.26	0.79	16.3
3	188	160	0.26	0.75	13.8
4	188	160	0.26	0.67	15.4
5	188	160	0.26	0.77	14.6
6	188	160	0.26	0.72	13.5
Average value	188	160	0.26	0.73	14.9

After six tests, the average width of the residual feed was 0.73 m, and the average value of the calculated transverse coefficient of variation was 14.9%, which was able to satisfy the auxiliary feeding needs of beef cattle breeding (width of scattered feed less than 0.75 m).

CONCLUSIONS

(1) Through theoretical analysis, device design and cattle farm tests, a supplemental feeding pusher was developed, which is more adaptable to cattle farms of different breeding scales and more suitable for intensive cattle farms.

(2) The three-factor, five-level orthogonal test established the regression model using test factors and evaluation indexes. The optimal combination of the working parameters was determined to be the screw shaft speed of 188 r/min, the sweeping roller brush speed of 160 r/min, and the traveling speed of 0.26 m/s, providing the basis for the selection of the machine working parameters of the supplemental feeding pusher.

(3) The test showed that the prototype machine had stable performance. The measured residual feed width was 0.73 m, the lateral coefficient of variation was 14.9%, and the test index met the needs of beef cattle auxiliary feeding. It can reduce the problem of high labor-intensity manual operation and effectively improve supplemental feeding and cleaning efficiency.

ACKNOWLEDGEMENT

This study was supported by the Shaanxi Livestock and Poultry Breeding Double-chain Fusion Key Project (2022GD-TSLD-46) and in part by SCO Institute of Modern Agricultural Development Program, Northwest A&F University.

REFERENCES

- [1] Alameer, A., Kyriazakis, I., Dalton, H. A., Miller, A.L. & Bacardit, J. (2020). Automatic recognition of feeding and foraging behavior in pigs using deep learning. *Biosystems Engineering*, 197, 91-104.
- [2] Álvarez-Rodríguez, J., Casasús, I., Blanco-Penedo, I., & Sanz, A. (2020). Effect of Feeding Level and Breed on the Daily Activity Budget of Lactating Beef Cows Fed Total Mixed Ration. *Agriculture*, 10(6), 195.
- [3] Bae, J., Park, S., Jeon, K., & Choi, J.Y. (2023). Autonomous System of TMR (Total Mixed Ration) Feed Feeding Robot for Smart Cattle Farm. *International Journal of Precision Engineering and Manufacturing*, 24, 423-433.

- [4] Bakirov, S.M., Logachev, O.V., & Shlyupikov, S.V. (2020). Justification of parameters of automatic control system of robot feed distribution in cattle barn. *IOP Conference Series Earth and Environmental Science*, 422, 12057.
- [5] Bisaglia, C., Belle Z., Berg, G.V. & Pompe, J.C. (2012). Automatic vs. conventional feeding systems in robotic milking dairy farms: a survey in The Netherlands. <https://www.researchgate.net/publication/267555832>.
- [6] Bisaglia, C., Lazzari, A., Giovinazzo, S., & Brambilla, M. (2023). Automatic Feeding Systems for Cattle in Italy: State of the Art and Perspectives. *AIIA 2022: Biosystems Engineering Towards the Green Deal*, 373-381.
- [7] Chen Z.J., Wang H.F., Zhou M.C., Zhu J., Chen J.H., & Li B. (2024) Design and Experiment of an Autonomous Navigation System for a Cattle Barn Feed-Pushing Robot Based on UWB Positioning. *Agriculture*, 14(5), 694.
- [8] Cummins, B., Kiely, P.O., Keane, M.G. & Kenny, D.A. (2009). Feed Intake Pattern, Behaviour, Rumen Characteristics and Blood Metabolites of Finishing Beef Steers Offered Total Mixed Rations Constituted at Feeding or Ensiling. *Irish Journal of Agricultural and Food Research*, 48, 57-73.
- [9] Da Borso, F., Chiumenti, A., Sigura, M., & Pezzuolo, A. (2017). Influence of automatic feeding systems on design and management of dairy farms. *Journal of Agricultural Engineering*, 48-52.
- [10] Greter, A.M., Miller-Cushon N.E.K., McBride, B.W., Widowski, T.M., Duffield, T.F. & DeVries T.J. (2015) Short communication: Limit feeding affects behavior patterns and feeding motivation of dairy heifers. *Journal of Dairy Science*, 98, 1248-1254.
- [11] Liu Y.F., Sun F.F., Wan F.C., Zhao H.B., Liu X.M., You W., Cheng H.J., Liu G. F., Tan X. W. & Song, E. L. (2016). Effects of Three Feeding Systems on Production Performance, Rumen Fermentation and Rumen Digesta Particle Structure of Beef Cattle. *Animal Bioscience*, 29, 659-665.
- [12] Mosquera, I. L. Q., Fierro, J. E. R., Zacarias, J. R. O., Montero, J. B., Quijano, S. A. C. & Huamanchahua, D. (2021). Design of an Automated System for Cattle-Feed Dispensing in Cattle-Cows. *2021 IEEE 12th Annual Ubiquitous Computing, Electronics & Mobile Communication Conference*, 671 - 675.
- [13] Moya, D., Mazzenga, A., Holtshausen, L., Cozzi, G., González, L. A., Calsamiglia, S., Gibb, D. G., McAllister, T. A., Beauchemin, K. A. & Schwartzkopf-Genswein, K. (2011). Feeding behavior and ruminal acidosis in beef cattle offered a total mixed ration or dietary components separately. *Journal of Animal Science*, 89(2), 520–530.
- [14] Pavkin, D.Y., Nikitin, E.A., Shilin, D.V., Belyakov, M.V., Golyshkov, I.A., Mikhailichenko, S. & Chepurina, E. (2023). Development Results of a Cross-Platform Positioning System for a Robotics Feed System at a Dairy Cattle Complex. *Agriculture*, 13(7), 1442.
- [15] Pavkin, D.Y., Shilin, D.V., Nikitin, E.A. & Kiryushin, I.A. (2021). Designing and Simulating the Control Process of a Feed Pusher Robot Used on a Dairy Farm. *Applied Science*, 11(22), 10665.
- [16] Nabokov, V. I., Novopashin, L. A., Denyozhko, L.V., Sadov, A. A., Ziablitskaia, N.V., Volkova, S.A., & Speshilova I.V. (2020). Applications of feed pusher robots on cattle farmings and its economic efficiency. *International Transaction Journal of Engineering Management & Applied Sciences & Technologies*, 2020,11(14): 14-20.
- [17] Tangorra, F. M. & Calcante, A. (2018). Energy consumption and technical-economic analysis of an automatic feeding system for dairy farms: Results from a field test. *Journal of Agricultural Engineering*, 49, 228-232.
- [18] Uzedhe, G.O., Akinloye, E.B.O. & Febaide, I.C. (2023). Development of an Animal Farm Robotic Feeding System. *Tropical Journal of Science and Technology*, 4(1), 14-22.
- [19] Yang L., Xiong B.H., Wang H., Chen R.P., & Zhao Y.G. (2022). Research Progress and Outlook of Livestock Feeding Robot (家畜饲喂机器人研究进展与发展展望). *Smart Agriculture*, 4(02):86-98.
- [20] Zhang Q., Ren H. L., & Hu J.H. (2023). Design and Experiment of Intelligent Feed-pushing Robot Based on Information Fusion (基于信息融合的智能推料机器人设计与试验), *Transactions of the Chinese Society for Agricultural Machinery*, 54(6):78-84.
- [21] Zhong R.Z., Zhao C.H., Feng P., Wang Y.T., Zhao X.L., Luo D.W., Cheng L., Liu D. & Fang Y. (2020) Effects of feeding ground versus pelleted total mixed ration on digestion, rumen function and milk production performance of dairy cows. *International Journal of Dairy Technology*, 73, 22-30.